Substrate Integrated Waveguide Filters Based on Dual-Mode Air-Filled Resonant Cavities

Cristiano Tomassoni, *Member, IEEE*, Lorenzo Silvestri, *Student Member, IEEE*, Anthony Ghiotto, *Senior Member, IEEE*, Maurizio Bozzi, *Fellow, IEEE*, and Luca Perregrini, *Fellow, IEEE*

***Abstract*—This paper presents the design and implementation of a novel class of substrate integrated waveguide (SIW) filters, based on partially air-filled cavity resonators. Removing the dielectric in a portion of the SIW cavity allows obtaining dual-mode cavities: such cavities represent a doublet, used as the building blocks in the design of filters. A thorough modal analysis of the air-filled resonant cavity based on transmission lines representation and a detailed study of the doublet permit to demonstrate a full control of the operation frequency, pass bandwidth, spurious-free region, and position of the transmission zeros of the filter. The paper presents the design, fabrication and measurement of several two-pole filters based on this concept, with the aim to show the capabilities of the proposed structure and of the design technique. A five-pole filter is also presented, to describe the extension of the proposed approach to higher order filters.**

***Index Terms*— Filters, Modal analysis, Resonator filters, Substrate integrated waveguide.**

I. INTRODUCTION

THE EVOLUTION OF THE WIRELESS MARKET with the advent of the Internet of Things (IoT) and the fifth generation mobile networks (5G) is driving the microwave community towards the investigation of novel technologies, able to support the needs of the emerging applications. In particular, the requirements of the next generation of wireless systems are low cost, simple design and easy fabrication, low loss and complete integration of entire wireless systems.

These emerging applications are stimulating the research in the field of the substrate integrated waveguide (SIW) technology [1]. Based on a dielectric substrate with top and bottom metal layers and two lateral rows of conductive vias, the SIW implements the classical rectangular waveguide in planar form. Due to its nature of planar structure, the SIW can be fabricated by using the same techniques of the microstrip line and coplanar waveguide circuits. On the other hand, due to its nature of rectangular waveguide, the SIW is shielded, thus preventing undesired radiation and spurious coupling, and presents lower losses than the microstrip line, due to the different electromagnetic field distribution.

Manuscript received 16 Aug. 2017; revised 16 Nov. 2017; accepted 7 Dec. 2017. This work has been partially supported under SPI2017 Young Investigator Training Program. This paper is an expanded version from the 2017 IEEE MTT-S International Conference on Numerical Electromagnetic and Multiphysics Modeling and Optimization, Seville, Spain, May 2017.

C. Tomassoni is with the University of Perugia, Department of Engineering, Perugia, Italy (e-mail: cristiano.tomassoni@unipg.it). L. Silvestri, M. Bozzi, and L. Perregrini are with the University of Pavia, Department of Electrical, Computer and Biomedical Engineering, Pavia, Italy (e-mail: lorenzo.silvestri01@ateneopv.it, maurizio.bozzi@unipv.it, luca.perregrini@unipv.it). A. Ghiotto is with the University of Bordeaux, IMS Laboratory, CNRS UMR 5218, IPB, 33405 Talence, France. (e-mail: anthony.ghiotto@ims-bordeaux.fr).

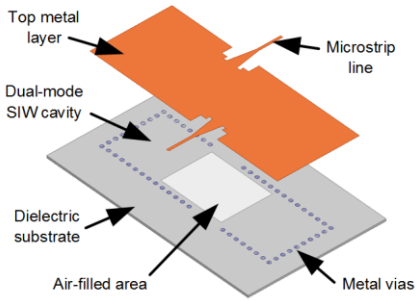

Fig. 1. Geometry of the two-pole band-pass filter (doublet) in air-filled SIW technology (from [19]).

SIW structures have been adopted for the design of a variety of microwave filters at different frequencies [2]-[7]. Size reduction and loss minimization are key points in the current research on SIW filters. Several alternative topologies have been proposed to reduce the footprint of SIW filters, including folded [8], half-mode [9], quarter-mode [10] and eighth-mode [6] SIW cavities. These solutions allow reducing the filter size by a factor ranging from two to eight. The price to pay is either a more complex fabrication based on a dual layer technology (in the case of the folded SIW), or higher radiation losses due to the partially open structure (in the case of half-mode and quarter-mode cavities). In the case of filters, the size reduction can also be achieved by using dual-mode resonators, which can also introduce transmission zeros by using the fundamental mode as a non-resonating mode [11]-[15]. When the main problem is the loss minimization, a possible solution is based on the air-filled SIW structure [16], [17]. In the air-filled SIW, the dielectric loss is reduced by removing part of the dielectric material inside the SIW, at the cost of a slightly larger size.

In this paper, a novel class of SIW filters is proposed, which combines the best features of dual-mode cavities and air-filled SIW (Fig. 1). By partially removing the dielectric material inside the SIW cavity, the resonance frequency of the first cavity modes can be controlled. This allows to achieve the desired frequency separation between the first and second

modes (used to define the pass band of the filter), as well as to maximize the resonance frequency of the higher modes (thus achieving maximum spurious-free bandwidth). The basic idea of this filter geometry was proposed in [18], where the air-filled SIW cavity is fed by an SIW line, and in [19], where the cavity is fed by a microstrip line. The basic concepts presented in the conference papers are widely extended here, with a thorough modal analysis of the air-filled cavity resonator allowing for the evaluation of resonant frequencies. Moreover, a detailed study of the dual-mode air-filled SIW cavity permits to demonstrate the full control of the operation frequency, pass bandwidth, spurious-free region, and position of the transmission zeros of the filter. Several prototypes of doublets are reported, to experimentally verify the proposed design strategy. Finally, the extension to higher order filters is shown by the design and experimental verification of a five-pole filter.

II. THEORY OF DUAL-MODE AIR-FILLED CAVITY

This section presents a theoretical analysis of a dual-mode air-filled cavity. A comprehensive understanding of this building block is necessary for the design of any structure based on such elementary resonator, including filters, as demonstrated in [18]-[19] and the following sections. In [18]-[19], time-consuming eigenmode simulations were used in the design steps. Instead, in this paper, an efficient transmission line theoretical model is used to derive a characteristic equation of the air-filled cavity. The partially air-filled cavity is divided in three homogeneous portions (a central air-filled part and two external dielectric filled parts), and each portion is described as a transmission line. The equivalent waveguide approximation [1] is adopted, and therefore a solid-wall rectangular cavity is considered. Finally, a transverse resonance technique is obtained to achieve the resonance modes of the overall (piecewise homogeneous) cavity. Namely, the solution of the characteristic equation provides a relation between the TM_{mn0} mode resonant frequencies and the cavity dimensions.

Fig. 2(*a*) represents an air-filled cavity of overall length A and width B. The height of the cavity is small compared to A and B, as it typically happens in SIW structures. The cavity is loaded with dielectric of relative permittivity ε_{r1} at its two ends, and it comprises a central air-filled region of relative permittivity $\varepsilon_{r0} = 1$ and length a. Fig. 2(*b*) shows the equivalent transmission line model of the cavity. The short-circuited dielectric loaded regions are represented by a homogeneous transmission line of length $l_1 = (A-a)/2$ with TM_{mn0} mode guide impedance Z_{1mn0}, propagation constant β_{1mn0} and dielectric permittivity $\varepsilon_{r1} > 1$.

The central air-filled region is modelled as two sections of length $l_0 = a/2$ with TM_{mn0} mode guide impedance Z_{0mn0}, propagation constant β_{0mn0} and dielectric permittivity $\varepsilon_{r0} = 1$. The guide impedance and propagation constant of both types of equivalent transmission lines are given by:

$$\beta_{0,1mn0} = \sqrt{\left(2\pi f\sqrt{\mu_0 \varepsilon_0 \varepsilon_{r0,1}}\right)^2 - \left(\frac{n\pi}{B}\right)^2} \qquad (1)$$

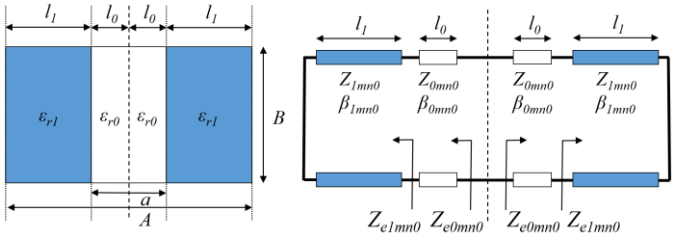

(*a*) (*b*)

Fig. 2. (*a*) Top view of an air-filled cavity resonator and (*b*) equivalent transmission-line model.

and

$$Z_{0,1mn0} = \sqrt{\frac{\mu_0}{\varepsilon_0\varepsilon_{r0,1} - \left(\frac{n}{2Bf\sqrt{\mu_0}}\right)^2}}, \qquad (2)$$

where f is the frequency, μ_0 is the vacuum permeability and ε_0 is the vacuum permittivity.

From transmission line theory, the Z_{e1mn0} equivalent impedance shown in Fig. 2(*b*) is determined by:

$$Z_{e1mn0} = jZ_{1mn0}\tan(\beta_{1mn0}l_1). \qquad (3)$$

Then, the equivalent impedance Z_{e0mn0} at the cavity symmetry plane looking toward one side is given by:

$$Z_{e0mn0} = Z_{0mn0}\frac{Z_{e1mn0} + jZ_{0mn0}\tan(\beta_{0mn0}l_0)}{Z_{0mn0} + jZ_{e1mn0}\tan(\beta_{0mn0}l_0)}. \qquad (4)$$

For odd modes (odd values of m), at the cavity resonance f_{TMmn0}, the imaginary part of (4) is:

$$\mathrm{Im}(Z_{e0mn0}) = \infty, \qquad (5)$$

whereas, for even modes (even values of m), at the cavity resonance f_{TMmn0}, the imaginary part of (4) is:

$$\mathrm{Im}(Z_{e0mn0}) = 0. \qquad (6)$$

To solve (5) and (6), the Newton–Raphson method can be used to determine the cavity resonance frequencies [20].

For illustration purposes, the following part will consider a total cavity length $A = 50$ mm and a dielectric material of permittivity $\varepsilon_{r1} = 10.5$. Fig. 3(*a*) and Fig. 3(*b*), reports the first four mode resonance frequencies obtained solving (5) and (6) of air-filled cavities of width $B = 19$ mm and 22.5 mm, respectively, versus the air-filled area length a. It can be observed that the mode resonance frequencies depend on both a and B dimensions. The first two modes (TM_{110} and TM_{210}) have very close resonant frequencies for a in the range of 10 mm to 35 mm. This is due to the fact that in the center of a dielectric-filled cavity the field of the TM_{110} mode is maximum, while that of the TM_{210} mode is null, as illustrated in Fig. 4(*a*). When the dielectric is removed in the central part of the cavity, this affects much more the TM_{110} mode than the TM_{210} mode, as shown in Fig. 4(*b*). Therefore, the resonance frequency of the TM_{110} mode increases much more than the one of the TM_{210} mode, thus decreasing the frequency separation between the two modes.

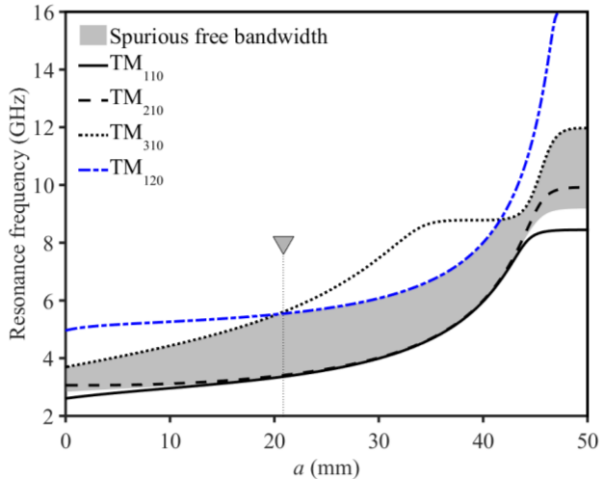

(*a*)

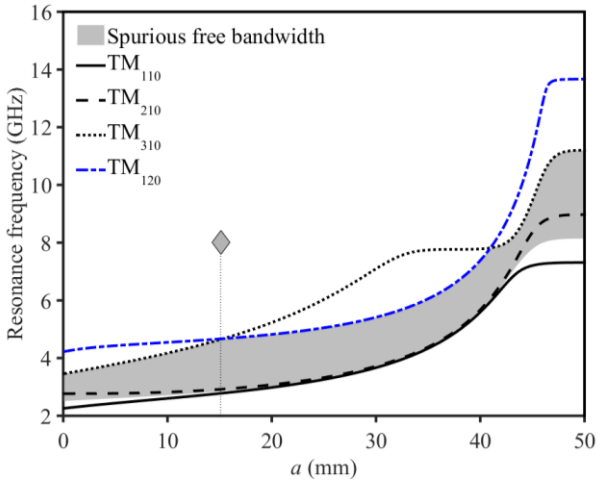

(*b*)

Fig. 3. Theoretical first four resonance frequencies and spurious free bandwidth versus dimension a (with $A = 50$ mm and $\varepsilon_{r1} = 10.5$): (*a*) For $B = 19$ mm; (*b*) For $B = 22.5$ mm.

Taking advantage of this characteristic, such air-filled cavity can be used for the design of a dual-mode cavity. By selecting the appropriate dimension a for a certain value of B, the relative frequency separation Δf between the TM_{110} and TM_{210} modes, given by:

$$\Delta f = \frac{2\,(f_{TM110} - f_{TM210})}{f_{TM110} + f_{TM210}}, \tag{7}$$

and illustrated in Fig. 5, can be selected. Lower relative frequency separation can be obtained using smaller value of B. It can be seen in Fig. 5 that the percent separation decreases until the dimension of the air-filled area is about $a = 35$ mm. Above that value, the cavity became similar to an hollow cavity, and the relative frequency separation increases significantly.

In Fig. 3, the third and fourth mode resonance frequencies are also shown. They limit the spurious-free bandwidth of the dual-mode cavity defined by the difference between the third mode resonance and the central frequency f_c of the dual-mode cavity given by:

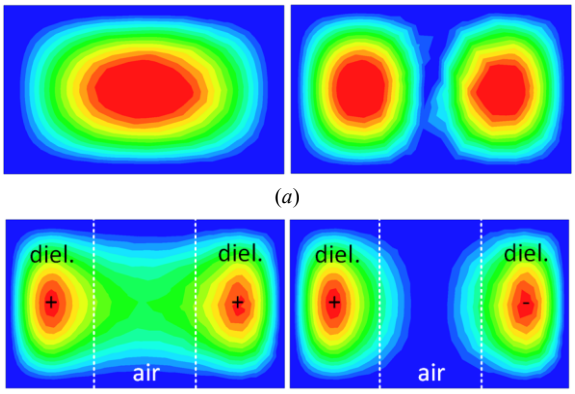

(*a*)

(*b*)

Fig. 4. Electric modal field of the first two resonant modes: (*a*) in dielectric-filled cavity; (*b*) in air-filled cavity.

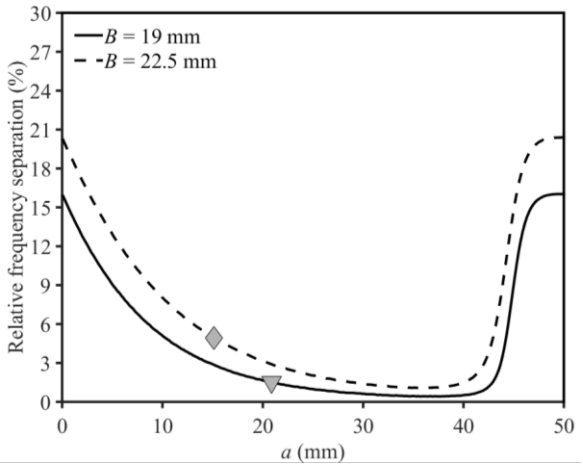

Fig. 5. Theoretical relative resonance frequency separation versus a dimension for $B = 19$ mm and 22.5 mm (with $A = 50$ mm and $\varepsilon_{r1} = 10.5$).

$$f_c = \frac{f_{TM110} + f_{TM210}}{2}. \tag{8}$$

It can be observed that, depending on the dimension a, the third resonance can be due to either the TM_{310} or the TM_{120} mode. The spurious-free bandwidth BW, relative to the central frequency f_c and given by:

$$BW = \frac{\min(f_{TM310}, f_{TM120}) - f_c}{f_c}, \tag{9}$$

is shown in Fig. 5 versus a. Optimum values are obtained for $a = 15.1$ mm and $B = 19$ mm (▼ marker) and $a = 20.85$ mm and $B = 22.5$ mm (♦ marker), respectively. These optimum values correspond to the smallest value a in Fig. 3, at which the TM_{120} mode become the third resonating mode.

Homogeneous cavities are obtained in the particular cases of $a = 0$ (empty cavity) and $a = 50$ mm (dielectric filled cavity). According to Fig. 5, in homogenous cavities, the frequency separation is maximum (it is the same in case of empty and dielectric filled cavity), and it also depends on B. This suggests that the frequency separation can be controlled also in homogenous waveguide by the ratio A/B. Unfortunately, according to Fig. 3, the frequency separation

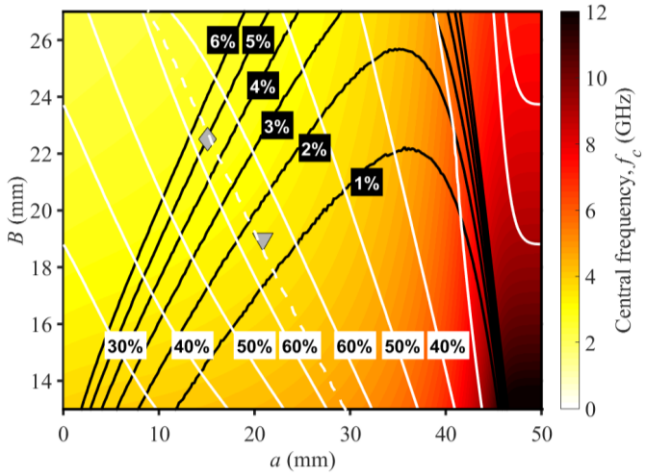

Fig. 6. Theoretical central frequency f_c with isocurves of the relative resonance frequency separation (black straight lines), relative spurious free bandwidth (white straight lines) and optimal relative spurious free bandwidth (white dotted line) versus dimensions a and B (A = 50 mm, ε_{r1} = 10.5).

between third and second mode is of the same magnitude of that of second and first mode. This can be easily verified by using the formula:

$$f_{mn0} = \frac{1}{2\pi\sqrt{\mu_0 \varepsilon_0 \varepsilon_r}} \sqrt{\left(\frac{m\pi}{A}\right)^2 - \left(\frac{n\pi}{B}\right)^2} \qquad (10)$$

for the evaluation of the resonance frequency of the resonant mode TM_{mn0}. This results in filters with very poor behaviour in terms of spurious free band.

Fig. 6 is a two-dimensional plot of the central frequency f_c versus dimensions a and B. It also shows isocurves of the relative resonance frequency separation (black straight lines) and relative spurious free bandwidth (white straight lines). The dimensions a and B also impact f_c. For a determined f_c and resonance frequency separation, two set of values a and B can be chosen. However, one of the two set provides a larger spurious-free bandwidth, and therefore it is more attractive for the design of a dual-mode cavity.

It can be observed in Fig. 6 that optimal relative spurious-free bandwidth (white dotted line) in excess of 60% with

TABLE I
DIMENSIONS AND THEORETICALLY OBTAINED CHARACTERISTICS OF THE SPURIOUS FREE BANDWIDTH OPTIMIZED 1.5% AND 5% RELATIVE FREQUENCY SEPARATION DUAL-MODE CAVITIES (ε_{r1}=10.5)

Two-resonance cavity	▼	♦
A (mm)	50	50
B (mm) | B/A	19 | 0.38	22.5 | 0.45
a (mm) | a/A	20.85 | 0.417	15.1 | 0.302
TM_{110} resonance frequency (GHz)	3.359	2.778
TM_{210} resonance frequency (GHz)	3.410	2.919
Relative frequency separation (%)	1.5	5
Central frequency, f_c (GHz)	3.385	2.849
First higher order mode resonance (GHz)	5.543	4.647
Relative spurious free bandwidth (%)	63.70	63.16

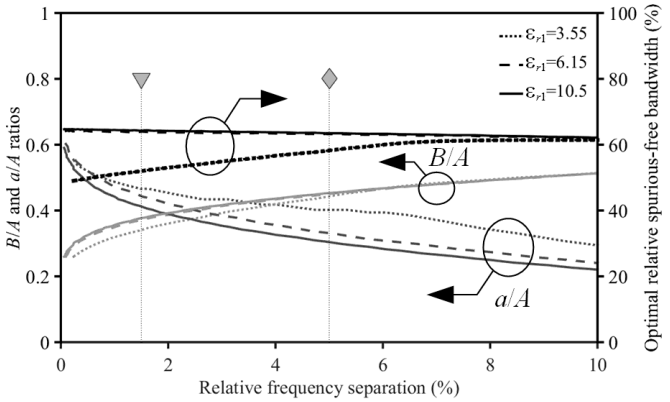

Fig. 7. Theoretical optimal spurious free bandwidth (black lines) and corresponding B/A ratio (dark gray lines) and a/A ratio (light gray lines) versus relative resonance frequency separation for ε_{r1} = 3.55, 6.15 and 10.5.

adjustable resonance frequency separation can be obtained properly choosing the dimensions a and B.

Table I summarizes the theoretically obtained characteristics of a set of two cavities with ε_{r1}=10.5, featuring 1.5% (identified in figures by a ▼ marker) and 5% (identified in figures by a ♦ marker) relative frequency separation in conjunction with the optimal relative spurious-free bandwidth.

The central frequency f_c of those optimal spurious free bandwidth dual-mode cavities can be adjusted varying the cavity overall length A while keeping constant the ratios B/A and a/A.

To achieve a desired relative resonance frequency separation, Fig. 7 provides the absolute optimal spurious-free bandwidth and corresponding ratios B/A and a/A for high, medium and low values of ε_{r1} (10.5, 6.15 and 3.55, respectively). Fig. 7 represents a diagram for the design of the air-filled cavity. For this reason, on the contrary of the previous figure where a fixed value of A is used, here all considered parameters are normalized with respect to A for sake of generality. It can be observed that optimal relative resonance frequency separation values of 65% to 62% can be obtained for all three substrates. And the higher the substrate permittivity is, the higher is the optimal a/A ratio and the lower is the optimal B/A ratio.

The procedure to design an optimal spurious-free bandwidth dual-mode cavity consists in selecting in Fig. 7 the dimensional ratios for a desired relative resonance frequency separation. Then the overall cavity length A is adjusted, while keeping constant ratios to obtain the desired central frequency f_c. Further design latitude could be offered synthesizing the desired εr_1 permittivity using either perforated substrates [21] or 3D printed materials [22].

III. DETAILED INVESTIGATION OF THE DOUBLET

This section describes the design strategy of a doublet based on the air-filled dual-mode SIW cavity. Such doublets are capable of two poles and two transmission zeros, with the possibility to locate zero very close to the pass-band. These doublets can be used as building blocks to obtain higher-order filters with high selectivity in the upper part of the band.

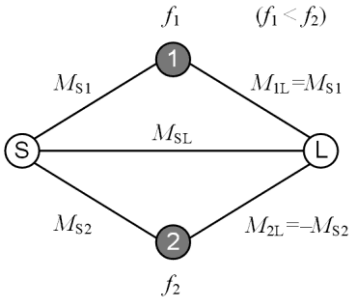

Fig. 8. Transversal topology of the doublet, implemented by using the air-filled dual-mode SIW cavity.

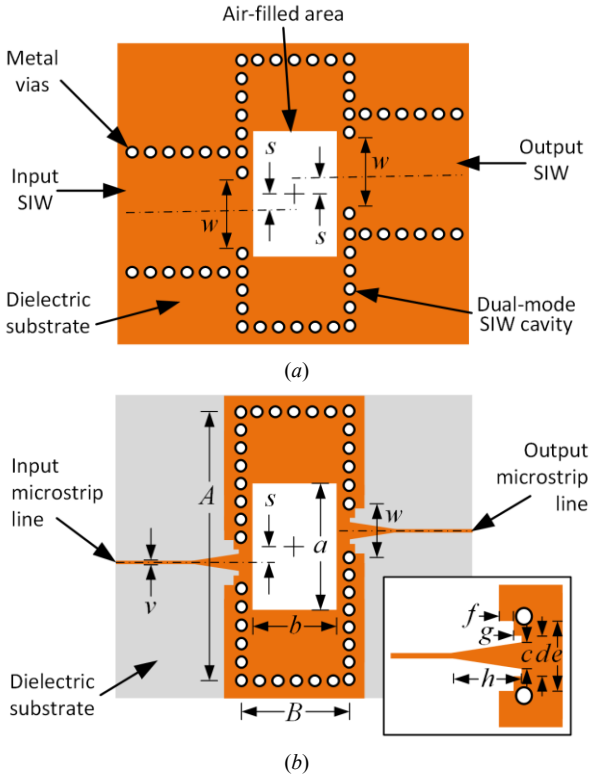

Fig. 9. Geometry of the doublet: (*a*) Fed by an SIW; (*b*) Fed by a microstrip.

A. Implementation of the Doublet

The air-filled dual-mode SIW cavity is exploited to implement the topology shown in Fig. 8. In this topology, the filter pass band mainly depends on the resonance frequencies f_1 and f_2 of the first two cavity modes and, as shown in the previous section, in the air-filled SIW they are fully controllable through the dimensions of the cavity.

The external excitation of the resonator (playing the role of source S and load L in the topology of Fig. 8) can be obtained by exploiting different guiding structures. In this paper, both SIW excitation (used in [18]) and microstrip excitation (used in [19]) are discussed.

Considering the SIW feeding illustrated in Fig. 9(*a*), the coupling to the first two resonant modes can be controlled by the inductive iris of width *w*. The larger the width *w*, the higher the couplings values M_{S1} and M_{S2}. In case of the microstrip feeding shown in Fig. 9(*b*), the coupling is mainly controlled by the microstrip taper (*c* and *h*) and the aperture of width *e*.

The implementation of the topology of Fig. 8 requires three coupling values with the same sign and the fourth with an opposite sign. For this reason, in the proposed structure, the SIW and microstrip feeding lines are positioned anti-symmetrically. According to Fig. 9 and considering the symmetric distribution of the fundamental mode electric field [Fig. 4(*b*), left], M_{S1} and M_{1L} couplings have the identical sign. Conversely, the asymmetric distribution of the second mode electric field [Fig. 4(*b*), right], leads to coupling values M_{S2} and M_{2L} with opposite sign.

In the considered topology, the capability to implement and control the first transmission zero is related to the possibility of adjusting the ratio M_{S1}/M_{S2}. In both SIW and microstrip feeding lines, this ratio can be tuned by the offset *s* shown in Fig. 9(*a*) and Fig. 9(*b*). A second transmission zero is obtained when the direct source-to-load coupling is present. Thanks to the proximity of input and output feeding lines, this coupling is present in the proposed resonator. In fact, proximity allows some power to directly flow from input to output through higher order modes, by-passing the resonant modes. The position of this second transmission zero is not easily controlled with the proposed geometry because of the lack of degrees of freedom.

B. Examples of Design of the Doublet

Starting from the partially air-filled dual mode cavities analyzed in Section II, some two-pole band-pass filters (doublets) have been designed, with the aim to show the full control of the relevant filter parameters.

The first doublet is based on the cavity with 1.5% relative frequency separation. The geometrical dimensions of the cavity in Table I have been used (except the transformation from effective dimensions to actual dimensions, according to the equivalent waveguide concept [1]). Only the input/output microstrip-to-SIW transitions have been optimized, in order to achieve 10 dB, 20 dB, and 30 dB pass-band input matching. The simulation results (from Ansys HFSS) are shown in Fig. 10. When the input matching is 10 dB, corresponding to a small external coupling, the position of the two poles of the frequency response, corresponding to the first two resonances of the cavity, are located at 3.355 GHz and 3.401 GHz, respectively. These values are almost coincident with the resonance frequencies of the cavity modes, reported in Table I (that are 3.359 GHz and 3.410 GHz). The resulting pass bandwidth is 1.36%. The first spurious pass band appears at 5.574 GHz, with a weak coupling of the mode supposed to resonate at 5.543 GHz in Table I. If the doublet is optimized for a better input matching, the external coupling increases, thus creating a modification of the cavity modes. Consequently, the relative frequency separation decreases, as shown in Fig. 10, and this effect needs to be accounted for in the filter design. Conversely, the spurious-free bandwidth and the position of the transmission zeros is practically unaffected by the modification of the external coupling (Fig. 10).

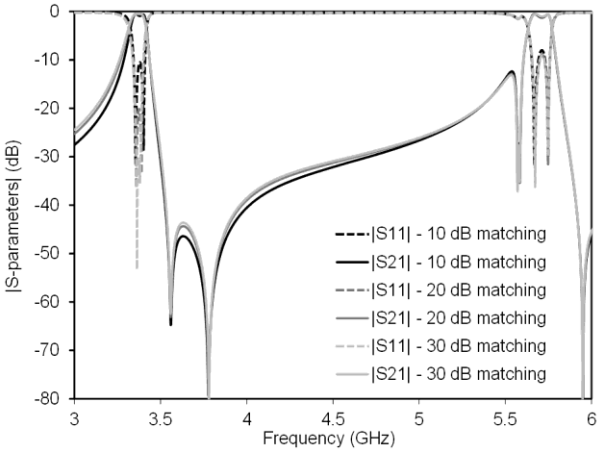

(*a*)

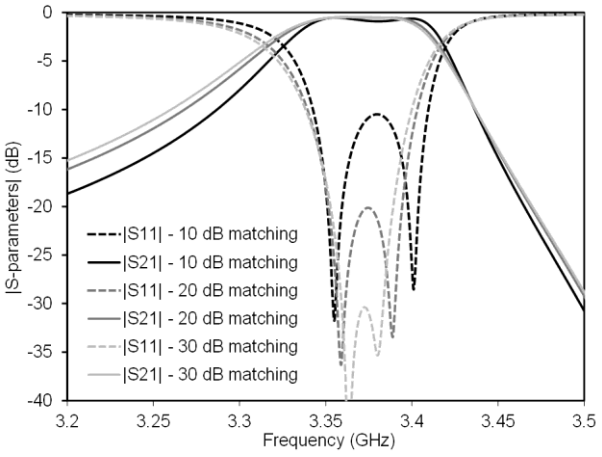

(*b*)

Fig. 10. Design of a two-pole filter with 1.5% relative pass bandwidth: (*a*) Wideband simulation of three cases, with 10 dB, 20 dB, and 30 dB input matching; (*b*) Detail of the pass band.

The filter with 20 dB input matching has been fabricated by milling technique on a dielectric laminate Taconic CER-10 (with relative dielectric permittivity ε_{r1}=10.5, loss tangent tanδ=0.0035, and thickness 1.27 mm). The photograph of the prototype is shown in Fig. 11(*a*), before the metallization of the metal vias by using conductive paste and the closing of the top/bottom air-filled area by copper sheets. The copper sheets at the top and bottom of the air-filled area have been applied and soldered as close as possible to the perforated region. Additional details on the technology of air-filled SIW structures can be found in [16]. The filter dimensions are reported in Table II, and the width of the input/output 50-Ω microstrip line is v=1.27 mm [Fig. 9(*b*)]. Measurements have been performed by using an Anritsu Universal Test Fixtures (UTF) 3680 and an Anritsu 37347C vector network analyzer (VNA). No de-embedding was applied to the measured results, to remove the connectors and transitions effect. The comparison between simulations and measurements is shown in Fig. 11(*b*). The measured insertion loss in the passband is 3.02 dB, compared to 2.04 dB in the simulation.

The same approach has been followed for the design of a second doublet, based on the cavity with 5.0% relative frequency separation, whose dimensions are shown in Table I.

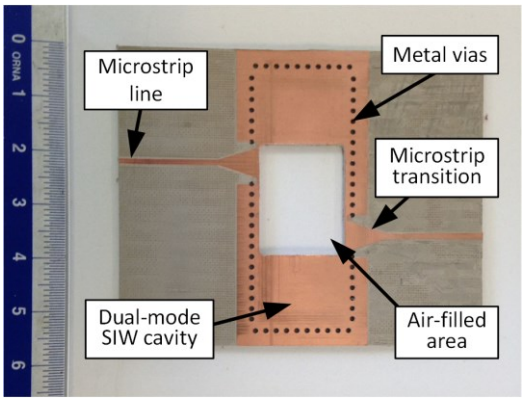

(*a*)

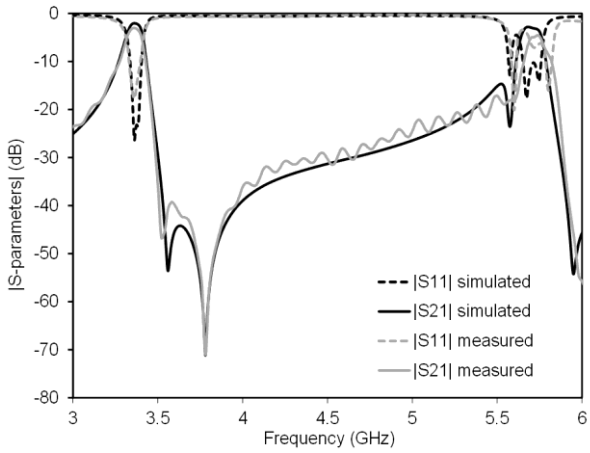

(*b*)

Fig. 11. Validation of the design of the two-pole filter with 1.5% relative pass bandwidth and 20-dB input matching: (*a*) Photograph of the prototype (before vias metallization and air-filled area covering); (*b*) Simulation and measurement of the frequency response of the filter.

TABLE II
DIMENSIONS OF THE FILTER WITH 1.5% RELATIVE FREQUENCY SEPARATION (IN MM)

A=50.54	B=19.54	a=21.39	b=16.54
c=5.85	d=7.85	e=8	f=3
g=1	h=7.85	s=7.05	w=8

Also in this case, the dimensions are not changes (with the exception of the transformation from equivalent waveguide to actual dimension). The transitions have been optimized for achieving a filtering function with 10 dB, 20 dB, and 30 dB input matching in the passband (Fig. 12). In the case of 10-dB matching (corresponding to weak external coupling), the poles of the frequency response appear at 2.664 GHz and 2.784 GHz, corresponding to a fractional bandwidth of 4.41%. If the filter is optimized to achieve a better input matching, the frequency separation decreases as in the previous example.

The filter with 20 dB input matching has been experimentally verified, by using the material, fabrication, and measurement technique previously described. The photograph of the prototype is shown in Fig. 13(*a*), and the filter dimensions are reported in Table III. The comparison between simulation and measurement frequency response is shown in Fig. 13(*b*), with an insertion loss of 1.45 dB in the measurement and of 0.88 dB in the simulation.

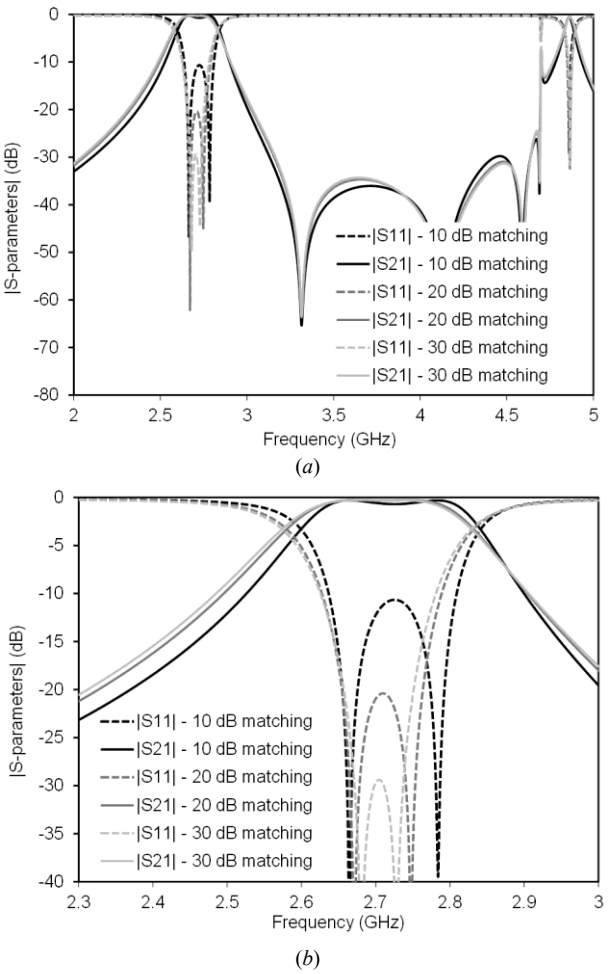

Fig. 12. Design of a two-pole filter with 5.0% relative pass bandwidth: (*a*) Wideband simulation of three cases, with 10 dB, 20 dB, and 30 dB input matching; (*b*) Detail of the pass band.

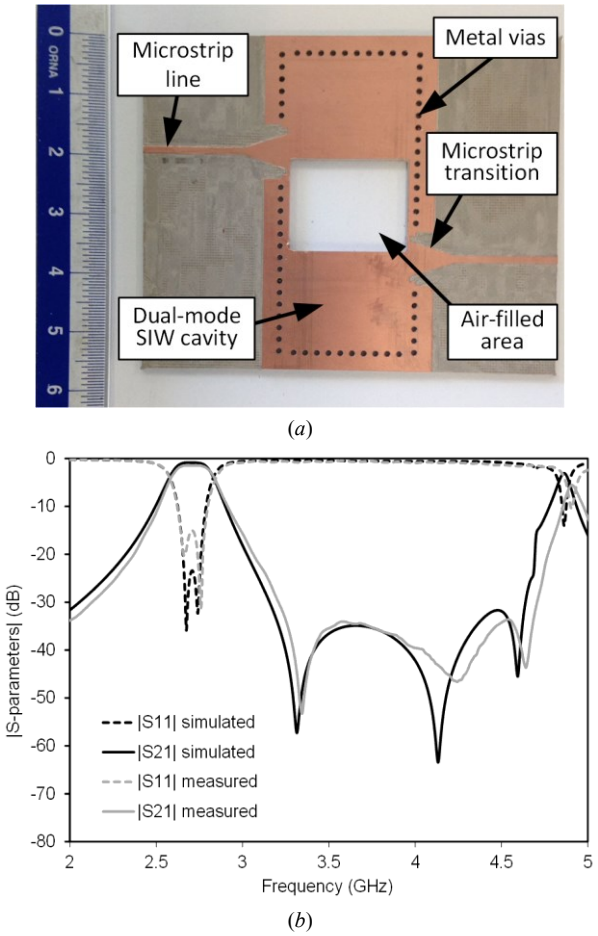

Fig. 13. Validation of the design of the two-pole filter with 5.0% relative pass bandwidth and 20-dB input matching: (*a*) Photograph of the prototype; (*b*) Simulation and measurement of the frequency response of the filter.

TABLE III
DIMENSIONS OF THE FILTER WITH 5% RELATIVE FREQUENCY SEPARATION (IN MM)

A=50.54	B=23.04	a=15.64	b=20.04
c=5.85	d=7.85	e=9	f=3
g=1	h=7.5	s=9.05	w=9

C. Control of the Transmission Zeros

As mentioned in Section III.A, the position of the first transmission zero depends on the ratio M_{S1}/M_{S2} and it can be tuned by modifying the offset s (Fig. 9). The position of the second transmission zero depends on the direct source-to-load coupling through higher-order cavity modes, and it is also affected by the offset s. In this section, some examples are reported, to demonstrate the full control of the transmission zeros in the doublet shown in Fig. 11.

If the position of the feeding lines is centered (s=0), only one mode of the cavity is excited by the microstrip line. As the field of the microstrip line has odd symmetry, the first cavity mode is excited and the second mode is not excited because of symmetry [Fig. 4(*b*)]. This results in a frequency response of the structure with one single pole [Fig. 14(*a*)]. The single transmission zero is due to the source-to-load coupling, which is particularly large in this case (due to proximity reasons).

Increasing the offset s of a small amount leads to the appearance of two poles (corresponding to the first two cavity modes) and two transmission zero, one of them very close to pass band [Fig. 14(*b*)]. Of course, modifying the offset s allows controlling the ratio between the couplings of the two modes as well as the direct source-to-load coupling. When s increases, the ratio M_{S1}/M_{S2} decreases, due to the modal field pattern [Fig. 4(*b*)], and the M_{SL} coupling also decreases, due to larger separation of the input and output ports. For this reason, the position of both transmission zeros are shifted in the same direction. Two more examples are shown in Fig. 14(*c*) and Fig. 14(*d*), where the value of s is larger and the transmission zeros are shifted far from the pass band.

In all these examples, the geometrical dimensions reported in Table II have been used, with the exception of the optimization of the microstrip transition (and, of course, the offset s).

The filter shown in Fig. 14(*d*) has been experimentally verified, with the fabrication and measurement described above. The photograph of the prototype is shown in Fig. 15(*a*), and the filter dimensions are reported in Table IV. The comparison between simulation and measurement frequency

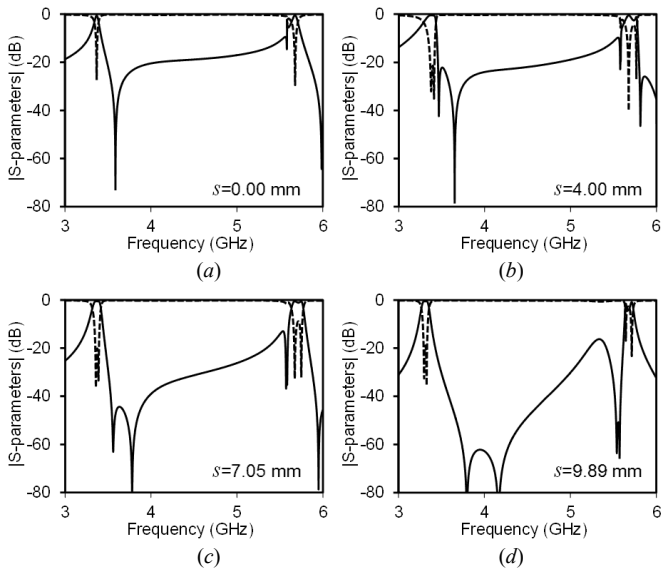

Fig. 14. Investigation of the control of the first transmission zero in the two-pole filter with 1.5% relative pass bandwidth and 20-dB input matching: (*a*) Symmetric structure; (*b*) Very close transmission zero; (*c*) Relatively close transmission zero; (*d*) Far transmission zero.

response is shown in Fig. 15(*b*), with an insertion loss of 2.91 dB in the measurement and of 2.21 dB in the simulation.

IV. DESIGN OF A HIGHER ORDER FILTER

Higher order filters can be obtained simply by cascading doublets through non-resonating nodes. This procedure allows for a modular design, where all cascaded doublets are first designed separately and then cascaded. Another advantage of this procedure is that the transmission zeros of each doublet are still present in the cascaded structure, and their position is preserved.

A simple way to implement non-resonating nodes is to use quarter-wave transmission line sections. The theory for the design of such filters has been presented in [13] and [15]. After the design, if necessary, it is possible to reduce the quarter-wave section by re-optimizing the whole filter to obtain a more compact structure.

Another possibility to cascade doublets consists in the use of half-wave sections [13]. The procedure is similar to the one based on quarter-wave sections. Modular design is still possible and position and number of doublet transmission zeros are still preserved after the cascade. The structure is larger than the one based on quarter-wave sections, but there is the advantage of obtaining an additional filter pole, being the half-wave section a resonator itself.

In order to demonstrate the feasibility of the proposed approach, a five-pole filter consisting of two doublets cascaded through a half-wave transmission line section has been designed and manufactured. The filter is centered at 2.875 GHz and its fractional bandwidth is 7.5%. The coupling matrix is provided in Fig. 16, whereas the relevant topology is shown in Fig. 17. According to Fig. 18(*a*), for the implementation of this topology, doublets with microstrip feeding on one side and SIW feeding on the other side have been selected. This allows the five-pole filter to be fed by microstrip lines, whereas the central resonator, consisting of half-wave transmission lines, is an SIW cavity, thus obtaining better performance in terms of losses.

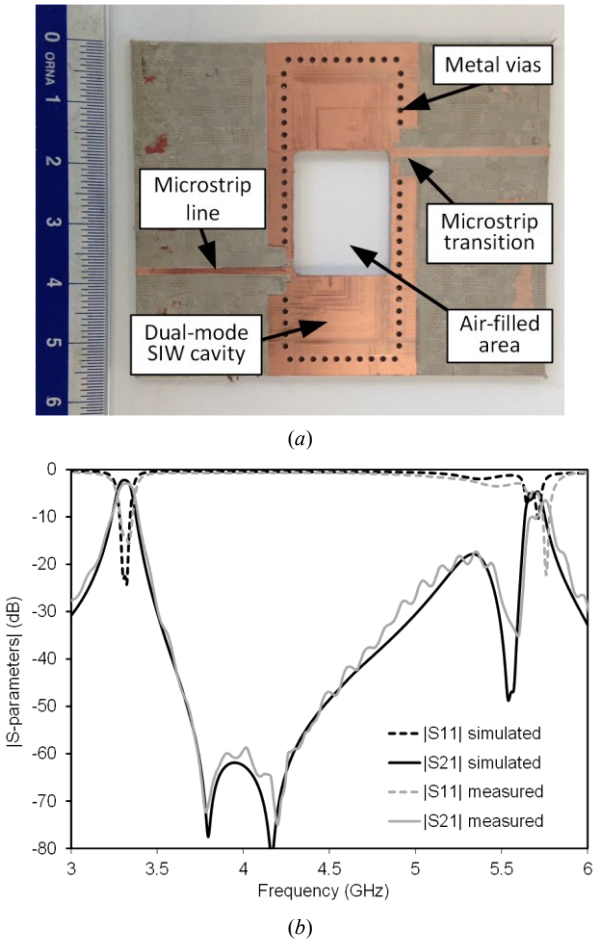

Fig. 15. Validation of the design of the two-pole filter with 1.5% relative pass bandwidth, 20-dB input matching, and far transmission zero: (*a*) Photograph of the prototype; (*b*) Simulation and measurement of the frequency response of the filter.

TABLE IV
DIMENSIONS OF THE FILTER WITH 1.5% RELATIVE FREQUENCY SEPARATION AND SETTING OF TRANSMISSION ZEROS (IN MM)

A=50.54	*B*=19.54	*a*=21.39	*b*=16.54
c=1.5	*d*=3.5	*e*=8	*f*=3
g=1	*h*=7.5	*s*=9.89	*w*=8

The manufactured prototype is shown in Fig. 18(*b*), while the relevant measured results are shown in Fig. 18(*c*), together with the full-wave simulation of the filter. Because of the symmetry of the filter, the two doublets are identical and each of them generate a transmission zero in the same position. After the cascade the position of the transmission zeros is maintained, thus resulting in a double zero in the upper stop-band. This double zero is very close to the filter band and guarantees a very high selectivity.

	S	1	2	3	4	5	L
S	0	0.949	0.509	0	0	0	0
1	0.949	0.506	0	0.799	0	0	0
2	0.509	0	-1.132	-0.056	0	0	0
3	0	0.799	-0.056	0.295	-0.056	0.799	0
4	0	0	0	-0.056	-1.132	0	0.509
5	0	0	0	0.799	0	0.506	0.949
L	0	0	0	0	0.509	0.949	0

Fig. 16. Coupling matrix of the five-pole filter, with FBW = 7.5% and central frequency at 2.875 GHz.

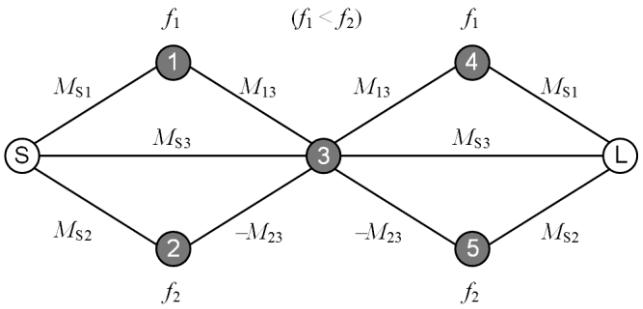

Fig. 17. Topology of the five-pole filter, based on two air-filled dual-mode SIW cavities and a standard SIW cavity.

V. CONCLUSION

This paper presents a novel class of substrate integrated waveguide filters, which combine the advantages of the dual-mode resonant cavities with the recently proposed air-filled SIW. The basic structure proposed in this work is a doublet, able to provide two poles and two zeros in the frequency response. A detailed investigation of the doublet demonstrated how to fully control the frequency response by modifying the geometrical dimensions. In particular, the length A of the cavity allows to set the operation frequency, the size a of the air-filled region determines the pass bandwidth, the width B of the cavity controls the out-of-band, and the offset s of the input/output lines sets the position of the transmission zeros. Several prototypes have been reported to show the validity of the proposed structure, including a five-pole filter that illustrates the extension of the concept to higher-order filters.

REFERENCES

[1] M. Bozzi, A. Georgiadis, and K. Wu, "Review of Substrate Integrated Waveguide (SIW) Circuits and Antennas," *IET Microwaves, Antennas and Propagation*, vol. 5, no. 8, pp. 909–920, June 2011.

[2] X. Chen and K. Wu, "Substrate Integrated Waveguide Filter: Basic Design Rules and Fundamental Structure Features," *IEEE Microw. Mag.*, vol. 15, no. 5, pp. 108–116, Jul./Aug. 2014.

[3] A. Pourghorban Saghati, A. Pourghorban Saghati and K. Entesari, "Ultra-Miniature SIW Cavity Resonators and Filters," *IEEE Trans. Microw. Theory Techn.*, vol. 63, no. 12, pp. 4329-4340, Dec. 2015.

[4] J. Schorer, J. Bornemann and U. Rosenberg, "Mode-Matching Design of Substrate Mounted Waveguide (SMW) Components," *IEEE Trans. Microw. Theory Techn.*, vol. 64, no. 8, pp. 2401-2408, Aug. 2016.

[5] P. Chu *et al.*, "Dual-Mode Substrate Integrated Waveguide Filter With Flexible Response," *IEEE Trans. Microw. Theory Techn.*, vol. 65, no. 3, pp. 824-830, Mar. 2017.

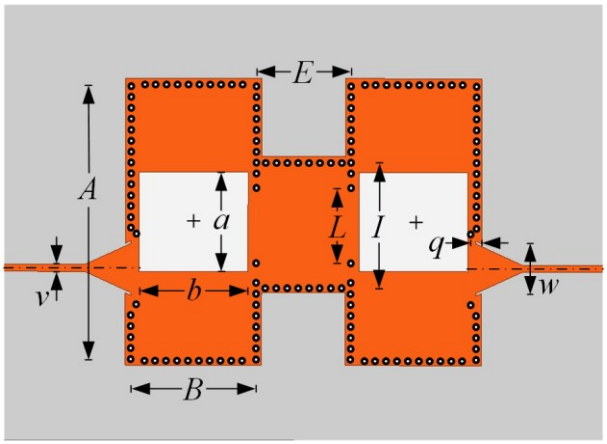

(*a*)

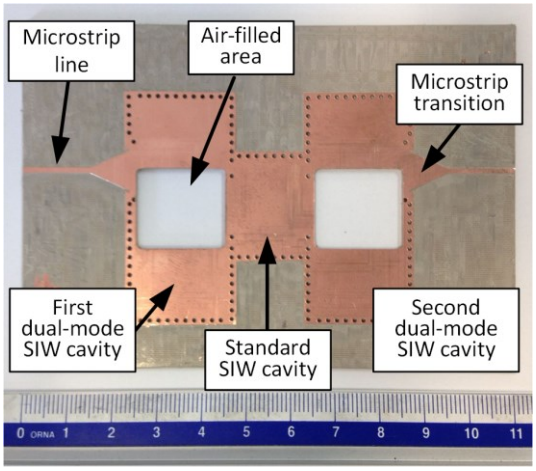

(*b*)

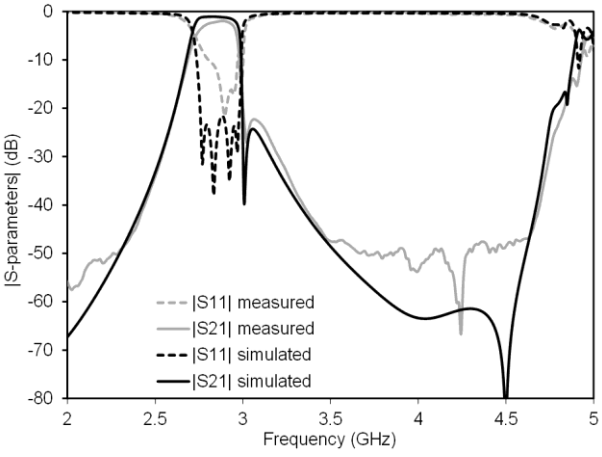

(*c*)

Fig. 18. Validation of the five-pole filter: (*a*) Geometry of the filter; (*b*) Photograph of the prototype; (*c*) Simulation and measurement of the frequency response of the filter.

TABLE V
DIMENSIONS OF THE FIVE-POLE FILTER (IN MM)

A=50.54	B=23.04	a=18.2	b=20.04
c=9	d=10	e=10	f=1
g=1	h=8.5	s=8	w=10
E=17.4	L=13.8	I=22.95	q=2

[6] P. Li, H. Chu, and R. S. Chen, "Design of Compact Bandpass Filters Using Quarter-Mode and Eighth-Mode SIW Cavities," *IEEE Trans. Compon. Packag. Manuf. Technol.*, vol. 7, no. 6, pp. 956-963, June 2017.

[7] M. Nosrati and M. Daneshmand, "Substrate Integrated Waveguide L-Shaped Iris for Realization of Transmission Zero and Evanescent-Mode Pole," *IEEE Trans. Microw. Theory Techn.*, vol. 65, no. 7, pp. 2310-2320, July 2017.

[8] R. Moro, S. Moscato, M. Bozzi, and L. Perregrini, "Substrate Integrated Folded Waveguide Filter with Out-of-Band Rejection Controlled by Resonant-Mode Suppression," *IEEE Microwave and Wireless Components Letters*, vol. 25, no. 4, pp. 214-216, April 2015.

[9] N. Delmonte, L. Silvestri, M. Bozzi, and L. Perregrini, "Compact Half-Mode SIW Cavity Filters Designed by Exploiting Resonant Mode Control," *International Journal of RF and Microwave Computer-Aided Engineering*, vol. 26, no. 1, pp. 72–79, Jan. 2016.

[10] S. Moscato, C. Tomassoni, M. Bozzi, and L. Perregrini, "Quarter-Mode Cavity Filters in Substrate Integrated Waveguide Technology," *IEEE Trans. Microw. Theory Techn.*, vol. 64, no. 8, pp. 2538-2547, Aug. 2016.

[11] C. Tomassoni, L. Silvestri, M. Bozzi, and L. Perregrini, "Substrate Integrated Waveguide Filters Based on Mushroom-Shaped Resonators," *International Journal of Microwave and Wireless Technologies*, vol. 8, no. 4-5, pp. 741-749, June 2016.

[12] S. Bastioli, C. Tomassoni, and R. Sorrentino, "TM Dual-Mode Pseudoelliptic Filters using Nonresonating Modes," *IEEE MTT-S 2010 International Microwave Symposium*, Anaheim, CA, 23-28 May 2010.

[13] C. Tomassoni, S. Bastioli, and R.V. Snyder, "Propagating Waveguide Filters Using Dielectric Resonators," *IEEE Trans. Microw. Theory Techn.*, vol. 63, no. 12, pp. 4366-4375, Dec. 2015.

[14] S. Bastioli and R. V. Snyder, "Waveguide evanescent mode filters using high-Q bypassed cavities for extreme close-in rejection," *44th European Microwave Conference*, pp. 175–178, Rome, Italy, Oct. 6–9, 2014.

[15] C. Tomassoni, S. Bastioli, and R.V. Snyder, "Compact Mixed-Mode Filter Based on TE_{101} Cavity Mode and $TE_{01\delta}$ Dielectric Mode," *IEEE Trans. Microw. Theory Techn.*, vol. 64, no. 12, pp. 4434-4443, Dec. 2016.

[16] F. Parment, A. Ghiotto, T. P. Vuong, J. M. Duchamp, and K. Wu, "Air-Filled Substrate Integrated Waveguide for Low-Loss and High Power-Handling Millimeter-Wave Substrate Integrated Circuits," *IEEE Trans. Microw. Theory Techn.*, vol. 63, no. 4, pp. 1228-1238, April 2015.

[17] F. Parment, A. Ghiotto, T. P. Vuong, J. M. Duchamp, and K. Wu, "Double Dielectric Slab-Loaded Air-Filled SIW Phase Shifters for High-Performance Millimeter-Wave Integration," *IEEE Trans. Microw. Theory Techn.*, vol. 64, no. 9, pp. 2833-2842, Sept. 2016.

[18] C. Tomassoni, L. Silvestri, A. Ghiotto, M. Bozzi, and L. Perregrini, "A Novel Filter Based on a Dual-Mode Air-Filled Substrate Integrated Waveguide Cavity Resonator," *2017 IEEE MTT-S International Conference on Numerical Electromagnetic and Multiphysics Modeling and Optimization for RF, Microwave, and Terahertz Applications* (NEMO2017), Sevilla, Spain, 17-19 May 2017.

[19] C. Tomassoni, L. Silvestri, M. Bozzi, L. Perregrini, and A. Ghiotto, "A dual-mode quasi-elliptic filter in air-filled substrate integrated waveguide technology," *47th European Microwave Conference* (EuMC), Nuremberg, Germany, 10-12 Oct. 2017.

[20] S. Adhikari, A. Ghiotto, and K. Wu, "Simultaneous electric and magnetic two-dimensionally tuned parameter-agile SIW devices," *IEEE Trans. Microw. Theory Techn.*, vol. 61, no. 1, pp. 423-435, Jan. 2013.

[21] L. Silvestri *et al*., "Substrate Integrated Waveguide Filters Based on a Dielectric Layer with Periodic Perforations," *IEEE Trans. Microw. Theory Techn.*, vol. 65, no. 8, pp. 2687–2697, Aug. 2017.

[22] E. Massoni *et al*., "3D-Printed Substrate Integrated Slab Waveguide for Single-Mode Bandwidth Enhancement," *IEEE Microwave and Wireless Components Letters*, vol. 27, no. 6, pp. 536-538, June 2017.

Cristiano Tomassoni (M'15) was born in Spoleto, Italy. He received the Laurea degree and Ph.D. degree in electronics engineering from the University of Perugia, Perugia, Italy, in 1996 and 1999, respectively. His disserta¬tion concerned the mode-matching analysis of discontinuities involving elliptical waveguides.

In 1999, he was a Visiting Scientist with the Lehrstuhl für Hochfrequenztechnik, Technical University of Munich, Munich, Germany, where he was involved with the modeling of waveguide structures and devices by using the generalized scattering matrix (GSM) technique. From 2000–2007, he was a Postdoctoral Research Associate with the University of Perugia. In 2001, he was a Guest Professor with the Fakultät für Elektrotechnik und Informationstechnik, Otto-von-Guericke University, Magdeburg, Germany. During that time, he was involved with the modeling of horn antennas having non-separable cross sections by using hybrid methods combining three different techniques: the finite-element method, mode-matching technique, and generalized multipole technique. He was also involved in the modeling of low-temperature co-fired ceramics by using the method of moments. He studied new analytical methods to implement boundary conditions in the transmission-line matrix method, and he modeled aperture antennas covered by dielectric radome by using spherical waves. Since 2007, he has been an Assistant Professor with the University of Perugia. Dr. Tomassoni is a member of the MTT-8 Filters and Passive Components Technical Committee of IEEE Microwave Theory and Technique Society (MTT-S). His main area of research concerns the modeling and design of waveguide devices and antennas. His research interests also include the development of reduced-size cavity filters, reconfigurable filters, and printed reconfigurable antenna arrays. Dr. Tomassoni was the recipient of the 2012 Microwave Prize presented by the IEEE Microwave Theory and Technique Society.

Lorenzo Silvestri (S'15) was born in Novara, Italy, in 1987. He received the Master degree in Electronic Engineering in 2014 at the University of Pavia. In 2014, he was an exchange student at the University of Ghent, Belgium. He is currently a Ph.D. student at the University of Pavia, Department of Computer, Electronics, and Biomedical Engineering. His main interests are related to the development of new components based on Substrate Integrated Waveguide (SIW) technology on innovative substrate materials. He was the recipient of the Best Paper Award at the 15th Mediterranean Microwave Symposium (MMS2015).

Anthony Ghiotto (S'05-M'09-SM'15) received the M.Sc. degree in 2005 and the Ph.D. degree in 2008 all in electrical engineering from the Grenoble Institute of Technology, Grenoble, France. He has been a Post-Doctoral fellow from 2009 to 2011 and a Research Associates from 2011 to 2012 in Pr. Ke WU team at the Poly-Grames Research Center from the École Polytechnique de Montréal, Montréal, QC, Canada. Since September 2012, Dr. Ghiotto holds an Assistant Professor position at the ENSEIRB-MATMECA engineering school from the Bordeaux Institute of Technology and the Laboratory of Integration from Materials to Systems (IMS) from the University of Bordeaux in Talence, France. His current research interests include the analysis, design and integration of microwave and millimeter wave passive and active circuits.

Dr. Ghiotto is a technical reviewer for the IEEE Transaction on Microwave Theory and Techniques, IEEE Microwave and Wireless Components Letters and the IEEE Antennas and Wireless Propagation Letters. Since 2017, he is the chair of the IEEE MTT French chapter.

Maurizio Bozzi (S'98–M'01–SM'12–F'18) was born in Voghera, Italy, in 1971. He received the Ph.D. degree in electronics and computer science from the University of Pavia, Pavia, Italy, in 2000.

He held research positions with various universities worldwide, including the Technische Universität Darmstadt, Germany; the Universitat de Valencia, Spain; and the École Polytechnique de Montréal, Canada. In 2002, he joined the Department of Electronics, University of Pavia, where he is currently an Associate Professor of electromagnetic fields (with Full Professor habilitation). He is also a Guest Professor of the Tianjin University (China) for the term 2015-2017.

He has authored or co-authored more than 100 journal papers and 260 conference papers. He co-edited the book *Periodic Structures* (Research Signpost, 2006) and co-authored the book *Microstrip Lines and Slotlines* (Artech House, 2013). His main research interests concern the computational electromagnetics, the substrate integrated waveguide technology, and the use of novel materials and fabrication technologies for microwave circuits (including paper, textile, and 3D printing).

Prof. Bozzi is an Elected Member of the Administrative Committee of the IEEE Microwave Theory and Techniques Society (MTT-S) for term 2017–2019 and the Chair of the Meeting and Symposia Committee of MTT-S AdCom for year 2018. He was the Secretary of IEEE MTT-S for year 2016 and a member of the General Assembly (GA) of the European Microwave Association (EuMA) from 2014 to 2016. He is an associate editor for the IEEE MICROWAVE AND WIRELESS COMPONENTS LETTERS, the IET Electronics Letters, and the IET Microwaves, Antennas and Propagation. He was the Guest Editor of special issues in the IEEE TRANSACTIONS ON MICROWAVE THEORY AND TECHNIQUES, the IEEE MICROWAVE MAGAZINE, and the IET Microwaves, Antennas and Propagation. He was the General Chair of the IEEE MTT-S International Microwave Workshop Series-Advanced Materials and Processes (IMWS-AMP 2017), in Pavia, Italy, 2017, of the IEEE International Conference on Numerical Electromagnetic Modeling and Optimization (NEMO2014), in Pavia, Italy, 2014, and of the IEEE MTT-S International Microwave Workshop Series on Millimeter Wave Integration Technologies, in Sitges, Spain, 2011.

He is Fellow of the IEEE (class of 2018). He received several awards, including the 2015 Premium Award for Best Paper in IET Microwaves, Antennas & Propagation, the 2014 Premium Award for the Best Paper in Electronics Letters, the Best Student Paper Award at the 2016 IEEE Topical Conference on Wireless Sensors and Sensor Networks (WiSNet2016), the Best Paper Award at the 15th Mediterranean Microwave Symposium (MMS2015), the Best Student Award at the 4th European Conference on Antennas and Propagation (EuCAP 2010), the Best Young Scientist Paper Award of the XXVII General Assembly of URSI in 2002, and the MECSA Prize of the Italian Conference on Electromagnetics (XIII RiNEm), in 2000.

Luca Perregrini (M'97-SM'12-F'16) was born in Sondrio, Italy, in 1964. He received the "Laurea" degree in Electronic Engineering and the Ph.D. in Electronics and Computer Science in 1989 and 1993, respectively. In 1992 he joined the Faculty of Engineering of the University of Pavia, he is currently full professor of electromagnetic fields and responsible of the Microwave Laboratory. He has been a visiting professor at the École Polytechnique de Montréal, Québec, Canada in 2001, 2002, 2005, and 2006.

He has been responsible of many research contracts with prominent international research centers and companies. His main research interests have been focused on the development of numerical methods for electromagnetics, and the design of microwave components and antennas. He authored or co-authored more than 90 journal papers and more than 250 conference papers, six book chapters, two textbooks, and co-edited the book Periodic Structures, (Research Signpost, 2006). His current research interests include the development of numerical methods for electromagnetics, and the design of microwave components and antennas.

Prof. Perregrini has been an invited speaker at many conferences, and has delivered invited seminar talks in Universities and research centers worldwide. He was a member of the General Assembly of the European Microwave Association (EuMA) from 2011 to 2013. He is a member of the Technical Committee MTT–15 (Microwave Field Theory) of IEEE Microwave Theory and Technique Society (MTT-S), of the Board of Directors of EuMA. He served as a member of prize committees for several conferences/societies.

He is Fellow of the Institute of Electrical and Electronics Engineers (IEEE). He was the co-recipient of several the best paper awards at international conferences. He is the appointed Technical Program Committee Chair of the International Microwave Workshop Series on Advanced Materials and Processes (IMWS-AMP 2017), Pavia, Italy, in 2017. He was the Technical Program Committee Chair of the IEEE MTT-S International Conference on Numerical Electromagnetic Modeling and Optimization (NEMO2014), Pavia, Italy, in 2014, and of the European Microwave Conference, Rome, Italy, in 2014. He was Associate Editor of the IEEE MICROWAVE AND WIRELESS COMPONENTS LETTERS from 2010 to 2013, of IEEE TRANSACTIONS ON MICROWAVE THEORY AND TECHNIQUES from 2013 to 2016, of the International Journal of Microwave and Wireless Technologies from 2011 to 2016, and of IET Electronic Letters from 2015 to 2016. He was Guest Editor of the IEEE TRANSACTIONS ON MICROWAVE THEORY AND TECHNIQUES in 2015 and of the International Journal of Microwave and Wireless Technologies in 2015.

He is currently Editor in Chief of the IEEE TRANSACTIONS ON MICROWAVE THEORY AND TECHNIQUES.